

respectively. Anal. Calcd for  $C_{13}H_{15}FeO_2PF_6$ : C, 38.61; H, 3.96; P, 7.67. Found: C, 38.85; H, 4.34; P, 7.55. IR spectrum (Nujol):  $\nu(\text{CO})$  2078 (s) and 2032 (s)  $\text{cm}^{-1}$ ;  $\nu(\text{C}=\text{C})$  1637 (w)  $\text{cm}^{-1}$ .  $^1\text{H}$  NMR (400 MHz,  $\text{CD}_3\text{COCD}_3$ ): 11,  $\delta$  1.00 (t, 3 H,  $\text{CH}_3$ ), 2.27 (m, 2 H,  $\text{CH}_2$ ), 3.42 (dd, 1 H,  $\text{H}^1$ ), 3.75 (dd, 1 H,  $\text{H}^2$ ), 5.4-5.5 (m, 2 H,  $\text{H}^3 + \text{H}^4$ ), 5.53 (s, 5 H,  $\text{C}_5\text{H}_5$ ), 6.57 (m, 1 H,  $\text{H}^5$ ),  $J_{13} = 14.7$  Hz,  $J_{12} = 1.4$  Hz,  $J_{23} = 8.3$  Hz,  $J_{45} = 14.5$  Hz,  $J_{5-\text{CH}_3} = 6.1$  Hz,  $J_{\text{CH}_2\text{CH}_3} = 6.4$  Hz; 12,  $\delta$  1.65 (d, 3 H,  $\text{CH}_3$ ), 2.50 (m, 1 H,  $\text{H}^4$ ), 2.95 (m, 1 H,  $\text{H}^5$ ), 3.36 (dd, 1 H,  $\text{H}^1$ ), 3.82 (dd, 1 H,  $\text{H}^2$ ), 4.92 (m, 1 H,  $\text{H}^3$ ), 5.30 (m, 1 H,  $\text{H}^7$ ), 5.51 (s, 5 H,  $\text{C}_5\text{H}_5$ ), 5.61 (m, 1 H,  $\text{H}^6$ ),  $J_{13} = 14.7$  Hz,  $J_{12} = 1.5$  Hz,  $J_{23} = 8.5$  Hz,  $J_{67} = 15.2$  Hz,  $J_{7-\text{CH}_3} = 6.2$  Hz.

**X-ray Diffraction Study of 5 and 8.** Data were collected at room temperature on a CAD4 diffractometer, using graphite-monochromated Mo  $K\alpha$  radiation. All data reduction and structure refinement were performed by using the NRCC-SDP-PDP-11 and NRCC-SDP-VAX packages (ORTEP from the Enraf-Nonius PDP 11/23 computer). Crystal data, details of data

collection, and structural analysis are summarized in Table V.

The structure of two compounds were solved by Patterson method. All non-hydrogen atoms were refined with anisotropic thermal parameters. All hydrogen atoms were added at idealized positions and included in the structure factor calculations.

**Acknowledgment.** We wish to thank the Chinese National Science Council for financial support of this work.

**Registry No.** 1, 103225-91-8; 2, 109716-86-1; 3, 96645-47-5; 4, 109638-07-5; 5, 109638-08-6; 6, 10938-09-7; 7, 109638-11-1; 8, 109638-06-4; 9, 109716-87-2; 10, 109638-13-3; 11, 109638-15-5; 12, 109638-17-7;  $\text{CpFe}(\text{CO})_2\text{Na}$ , 12152-20-4; (*E,E*)-1-chlorohexa-2,4-dione, 34632-89-8.

**Supplementary Material Available:** Figure 3, structure of the  $\text{PF}_6$  anion (3 pages); listings of structure factors for 5 and 8 (34 pages). Ordering information is given on any current masthead page.

## Reactions of $(\text{Me}_3\text{SiCH}_2)_2\text{AsSiMe}_3$ with Gallium Halides. Crystal Structure and Dynamic NMR Study of the Dimer $\{[(\text{Me}_3\text{SiCH}_2)_2\text{As}]_2\text{GaBr}\}_2$

Andrew P. Purdy, Richard L. Wells,\* Andrew T. McPhail, and Colin G. Pitt\*

Department of Chemistry, Paul M. Gross Chemical Laboratory, Duke University, Durham, North Carolina 27706

Received January 23, 1987

$(\text{Me}_3\text{SiCH}_2)_2\text{AsSiMe}_3$  reacted with the gallium halides  $\text{GaBr}_3$ ,  $\text{MeGaCl}_2$ , and  $\text{PhGaCl}_2$  to produce the (arsino)gallanes  $[(\text{Me}_3\text{SiCH}_2)_2\text{AsGaBr}_2]_3$ ,  $\{[(\text{Me}_3\text{SiCH}_2)_2\text{As}]_2\text{GaBr}\}_2$ ,  $[(\text{Me}_3\text{SiCH}_2)_2\text{AsGaMeCl}]_n$  ( $n = 2, 3$ ), and  $[(\text{Me}_3\text{SiCH}_2)_2\text{AsGaCIPh}]_n$  ( $n = 2, 3$ ), which were characterized by elemental analysis (C and H),  $^1\text{H}$  and  $^{13}\text{C}$  NMR spectroscopy, and cryoscopic molecular weight determinations. A single-crystal X-ray diffraction study of  $\{[(\text{Me}_3\text{SiCH}_2)_2\text{As}]_2\text{GaBr}\}_2$  was carried out. Crystal data are as follows: triclinic, space group  $P\bar{1}$ ,  $a = 11.892$  (2) Å,  $b = 12.492$  (2) Å,  $c = 11.515$  (1) Å,  $\alpha = 98.24$  (1)°,  $\beta = 113.57$  (1)°,  $\gamma = 84.21$  (1)°,  $V = 1549.9$  Å<sup>3</sup>,  $Z = 1$ . The centrosymmetric, dimeric molecule crystallizes in the trans configuration, with unequal endocyclic Ga-As distances [2.513 (1) Å and 2.521 (1) Å] and very significantly different bond angles [84.37 (1)° and 95.63 (2)°, respectively, at Ga and As] in the planar (Ga-As)<sub>2</sub> ring. The Ga-exo-As distance of 2.437 (1) Å is the shortest yet measured in an organogallium-arsenic compound. A  $^{13}\text{C}\{^1\text{H}\}$  dynamic NMR study of  $\{[(\text{Me}_3\text{SiCH}_2)_2\text{As}]_2\text{GaBr}\}_2$  revealed that both an interchange of the  $(\text{Me}_3\text{SiCH}_2)_2\text{As}$  groups [ $\Delta H^\ddagger = 18.7 \pm 0.3$  kcal/mol;  $\Delta S^\ddagger = 4.5 \pm 1.0$  cal/(mol K)] and a trans-cis isomerization [ $\Delta H^\ddagger = 17.4 \pm 0.7$  kcal/mol;  $\Delta S^\ddagger = -2.2 \pm 2.1$  cal/(mol K)] take place.

### Introduction

Prior to our recent studies,<sup>1</sup> the only method of preparing organogallium-arsenic compounds was that reported by Coates et al.<sup>2</sup> These authors prepared two mono(arsino)gallanes by the cleavage of a single Ga-C bond in  $\text{Me}_3\text{Ga}$  with the As-H bond of a secondary arsine. In our hands, this reaction not only suffered a reduction in efficiency but also eventually failed to yield the desired

products as the substituents on Ga and As increased in size.<sup>1a</sup> Moreover, the fact that bis- and tris(arsino)gallanes could not be made by this route<sup>1a</sup> led us to examine alternative methods of forming the Ga-As bond, viz., the coupling of gallium chlorides with lithium arsenides<sup>16g</sup> or silyl arsines.<sup>1a</sup> Others have since reported the use of the lithium arsenide method.<sup>3</sup> There is ample precedent for the reaction of silyl-substituted main-group elements (E-SiMe<sub>3</sub>) with covalent halides  $\text{MCl}_x$  to yield an E-M bond and  $\text{Me}_3\text{SiCl}$ .<sup>4</sup> Our previous communication<sup>1a</sup> revealed that secondary trimethylsilylarsines,  $\text{R}_2\text{AsSiMe}_3$ , readily

(1) (a) Pitt, C. G.; Purdy, A. P.; Higa, K. T.; Wells, R. L. *Organometallics* 1986, 5, 1266. (b) Wells, R. L.; Purdy, A. P.; McPhail, A. T.; Pitt, C. G. *Abstracts of Papers*, 189th Meeting of the American Chemical Society, Miami Beach, FL; American Chemical Society: Washington, DC, 1985; INOR 26. (c) Wells, R. L.; Purdy, A. P.; McPhail, A. T.; Pitt, C. G. *J. Chem. Soc., Chem. Commun.* 1986, 487. (d) Wells, R. L.; Purdy, A. P.; McPhail, A. T.; Pitt, C. G. *J. Organomet. Chem.* 1986, 308, 281. (e) Pitt, C. G.; Higa, K. T.; McPhail, A. T.; Wells, R. L. *Inorg. Chem.* 1986, 25, 2483. (f) Wells, R. L.; Purdy, A. P.; Higa, K. T.; Pitt, C. G. *Abstracts of Papers*, XX Organosilicon Symposium, Tarrytown, NY, April 1986; p-2.27. (g) Wells, R. L.; Purdy, A. P.; Higa, K. T.; McPhail, A. T.; Pitt, C. G. *J. Organomet. Chem.* 1987, 325, C7.

(2) (a) Coates, G. E.; Graham, J. J. *J. Chem. Soc.* 1963, 233. (b) Beachley, O. T.; Coates, G. E. *J. Chem. Soc.* 1965, 3241.

(3) Arif, A. M.; Benac, B. L.; Cowley, A. H.; Geerts, R.; Jones, R. A.; Kidd, K. B.; Power, J. M.; Schwab, S. T. *J. Chem. Soc., Chem. Commun.* 1986, 1543.

(4) See, for example: (a) Abel, E. W.; Armitage, D. A.; Willey, G. R. *J. Chem. Soc.* 1965, 57. (b) Wells, R. L.; Collins, A. L. *Inorg. Chem.* 1966, 5, 1327. (c) Abel, E. W.; Illingsworth, S. M. *J. Chem. Soc. A* 1969, 1094. (d) Harman, J. S.; McCartney, M. E.; Sharp, D. W. A. *J. Chem. Soc. A* 1971, 1547. (e) Goetze, R.; Noeth, H. Z.; *Z. Naturforsch., B: Anorg. Chem., Org. Chem., Biochem., Biophys., Biol.* 1975, 30B, 875. (f) Nutt, W. R.; Stimson, R. E.; Leopold, M. F.; Rubin, B. H. *Inorg. Chem.* 1982, 21, 1909. (g) Hoffman, G. G. *J. Organomet. Chem.* 1984, 273, 187.

react with  $\text{GaCl}_3$  in a 1:1 or 2:1 ratio to produce compounds of the form  $(\text{R}_2\text{AsGaCl}_2)_n$  and  $[(\text{R}_2\text{As})_2\text{GaCl}]_n$ . When the 3:1 stoichiometry was also investigated, replacement of all chlorine atoms was observed when  $\text{R} = \text{mesityl}$ , but not when  $\text{R} = \text{Me}_3\text{SiCH}_2$ . Furthermore, we demonstrated that the molecule  $\{[(\text{Me}_3\text{SiCH}_2)_2\text{As}]_2\text{GaCl}\}_2$  is fluxional and undergoes an exchange of the endocyclic and exocyclic  $\text{R}_2\text{As}$  groups.

In this paper we describe the reaction of  $(\text{Me}_3\text{SiCH}_2)_2\text{AsSiMe}_3$  (1) with  $\text{GaBr}_3$ , the first crystal structure of a bis(arsino)gallane,  $\{[(\text{Me}_3\text{SiCH}_2)_2\text{As}]_2\text{GaBr}\}_2$ , along with a dynamic NMR study of this compound, and the results of treating 1 with other gallium halides.

### Experimental Section

**General Information.** All manipulations were carried out either in a Vacuum/Atmospheres HE-43 Dri-Lab or in Schlenk apparatus under dry nitrogen. All solvents except ligroin were distilled from sodium benzophenone ketyl under nitrogen. Ligroin (bp 95–110 °C, Eastman) was distilled from stirred molten sodium under nitrogen.  $\text{GaBr}_3$  was obtained from Alfa Products and D. F. Goldsmith Chemical & Metal Corp.;  $\text{GaCl}_3$  was purchased from Eagle-Picher Corp.;  $\text{MeGaCl}_2$ ,<sup>5a</sup>  $\text{PhGaCl}_2$ ,<sup>5b</sup> and  $(\text{Me}_3\text{SiCH}_2)_2\text{AsSiMe}_3$ <sup>1a</sup> were prepared by published procedures. Crystals used in the X-ray analysis were flame sealed in 0.5-mm glass capillaries, and NMR tubes were sealed under vacuum. Proton NMR spectra were recorded by using 5-mm tubes on either an IBM NR-80 80-MHz spectrometer, a Bruker WM-250 250-MHz spectrometer, or a Varian XL-300 300-MHz spectrometer. The latter was used to obtain all variable-temperature  $^1\text{H}$  and  $^{13}\text{C}\{^1\text{H}\}$  spectra. Some other  $^{13}\text{C}\{^1\text{H}\}$  spectra were recorded on a JEOL FX-90Q spectrometer at 22.5 MHz. The spectra were referenced to TMS, using the residual protons or the carbons of the deuterated solvents as the chemical shift reference: for  $^1\text{H}$ ,  $\text{C}_6\text{D}_6$   $\delta$  7.15,  $\text{C}_6\text{D}_6\text{CD}_2\text{H}$  2.09; for  $^{13}\text{C}$ ,  $\text{C}_6\text{D}_6$  128.0,  $\text{C}_6\text{D}_5\text{CD}_3$  20.4. Molecular weights were obtained cryoscopically in benzene or cyclohexane with a Normag 2029 apparatus. All melting points (uncorrected) were obtained with a Thomas-Hoover Uni-melt apparatus and flame-sealed capillaries. Elemental analyses were performed by E+R Microanalytical Laboratory, Inc., Corona, NY.

$\{[(\text{Me}_3\text{SiCH}_2)_2\text{AsGaBr}_2]\}_3$  (2).  $\text{GaBr}_3$  (0.43 g, 1.4 mmol) was dissolved in ca. 15 mL of warm pentane, and the mixture was allowed to cool before a pentane solution (ca. 5 mL) of 1 was quickly added (0.45 g, 1.4 mmol). The solution was cloudy for less than a minute and then cleared. After 12 h many large colorless crystals had separated from solution. Three days later, the mother liquor was removed and the crystals were dried under vacuum (0.54 g, 87% yield), mp 210–219 °C. Anal. Calcd (Found) for  $\text{C}_{24}\text{H}_{66}\text{Si}_6\text{As}_3\text{Ga}_3\text{Br}_9$ : C, 20.06 (20.33); H, 4.63 (4.83). Mol wt (cryoscopic, 0.524 g in 17.75 g of benzene) 1436 (1443  $\pm$  131). NMR:  $^1\text{H}$  ( $\text{C}_6\text{D}_6$ , 299.943 MHz)  $\delta$  0.26 (s,  $\text{SiMe}_3$ ), 1.85 (s,  $\text{CH}_2$ );  $^{13}\text{C}\{^1\text{H}\}$  ( $\text{C}_6\text{D}_6$ , 75.429 MHz)  $\delta$  1.73 (s,  $\text{SiMe}_3$ ), 8.84 (s,  $\text{CH}_2$ ).

$\{[(\text{Me}_3\text{SiCH}_2)_2\text{As}]_2\text{GaBr}\}_2$  (3). A saturated solution of  $\text{GaBr}_3$  (0.48 g, 1.6 mmol) in ca. 10 mL of pentane was added to a pentane solution of 1 (1.0 g, 3.1 mmol). The mixture became cloudy and then largely cleared, but a few flakes did not dissolve (presumably impurities in the  $\text{GaBr}_3$ ). Benzene was added, and the mixture was filtered. After 2 days, the volatiles were removed in vacuo from the filtrate. The resulting off-white partial solid was crystallized from several milliliters of warm (55 °C) ligroin. The mother liquor was decanted and the colorless crystals dried in vacuo (0.30 g, 30%), mp 90–121 °C (dec). Anal. Calcd (Found) for  $\text{C}_{32}\text{H}_{88}\text{Si}_8\text{Ga}_2\text{Br}_2$ : C, 29.64 (29.72); H, 6.84 (7.01). Mol wt (cryoscopic, 0.280 g in 13.54 g of cyclohexane) 1297 (1260  $\pm$  39). NMR:  $^1\text{H}$  (299.943 MHz,  $\text{C}_6\text{D}_5\text{CD}_3$ ) *trans*-3  $\delta$  0.26, 0.24 (s,  $\text{SiMe}_3$ ), 1.65 and 1.70  $^2J_{\text{HH}} = 13.9$  Hz (AB pattern, endo), 0.95 and 1.78  $^2J_{\text{HH}} = 13.6$  Hz (AB pattern, exo); *cis*-3 1.00 and 1.57  $^2J_{\text{HH}} = 13.5$  Hz (AB pattern, exo), 1.59, 1.86 (s, endo) ( $\text{CH}_2\text{As}$ ), 0.22 ( $\text{Me}_3\text{Si}^?$ ), the  $\text{Me}_3\text{Si}$  peaks of *cis*-3 appear to be hidden under the *trans* peaks;  $^1\text{H}$  (299.943 MHz,  $\text{C}_6\text{D}_6$ ) *trans*-3 0.26 ( $\text{SiMe}_3$ ), 1.00 and 1.84  $^2J_{\text{HH}} = 13.6$  Hz (AB pattern, exo), 1.68 and 1.75  $^2J_{\text{HH}} = 14.1$  Hz (AB pattern, endo) ( $\text{CH}_2\text{As}$ ); *cis*-3 0.23, 0.24 ( $\text{Me}_3\text{Si}$ ), 1.06, and

1.62  $^2J_{\text{HH}} = 13.5$  Hz (AB pattern, exo), 1.59 (endo), 1.93 (endo) ( $\text{CH}_2\text{As}$ );  $^{13}\text{C}\{^1\text{H}\}$  (75.429 MHz,  $\text{C}_6\text{D}_5\text{CD}_3$ ) *trans*-3 0.19 (exo), 1.35 (endo) ( $\text{SiMe}_3$ ), 8.95 (exo), 9.77 (endo) ( $\text{CH}_2\text{As}$ ); *cis*-3 0.36 (exo), 1.42 (endo) ( $\text{SiMe}_3$ ), 9.19 (exo), 9.69 (endo), 11.13 (endo) ( $\text{CH}_2\text{As}$ ).

$\{[(\text{Me}_3\text{SiCH}_2)_2\text{AsGaClMe}]\}_2$  (4).  $\text{MeGaCl}_2$  (0.18 g, 1.2 mmol) and 1 (0.36 g, 1.1 mmol) were combined in pentane in a 25-mL Pyrex bulb with a stopcock. The pentane was evaporated under vacuum, and the mixture was warmed gently for 1 day. All volatiles were then removed, leaving a white solid, mp 79–81 °C. Anal. Calcd (Found) for  $\text{C}_9\text{H}_{25}\text{Si}_2\text{AsGaCl}$ : C, 29.25 (29.26); H, 6.82 (6.66). Mol wt (cryoscopic, 0.166 g in 11.42 g of cyclohexane) 369.58n (1010  $\pm$  12;  $n = 2.73$ ). NMR:  $^{13}\text{C}\{^1\text{H}\}$  (75.429 MHz,  $\text{C}_6\text{D}_6$ )  $\delta$  7.40, 7.29, 7.17, 6.86, 6.76, 6.60, 6.48, 6.36 ( $\text{CH}_2$ ), 1.84, 1.64, 1.55, 1.42, 1.29, 1.09, 0.92, 0.86, 0.71, 0.06, -0.04, -0.62 ( $\text{Me}_3\text{Si}$  and  $\text{MeClGa}$ ).

**NMR Equilibrium Study of 4.** Sealed 5-mm NMR tubes containing three different concentrations of 4 in toluene- $d_8$  [(A) 0.0068/n M, (B) 0.0829/n M, (C) 0.345/n M] were prepared and kept at 25.0 °C for 6 days. The predominant species was identified as the *trans* trimer by its distinctive pattern ( $^1\text{H}$ , 300 MHz):  $\delta$  0.179 (9 H), 0.200 (18 H), 0.215 (18 H), 0.260 (9 H) (s,  $\text{SiMe}_3$ ), 0.585 (6 H), 0.577 (3 H) (s,  $\text{GaClMe}$ ), 1.330 (s, 2 H), 1.290 and 1.511  $^2J_{\text{HH}} = 13.8$  Hz (AB pattern, 4 H), 1.433 and 1.626  $^2J_{\text{HH}} = 13.9$  Hz (AB pattern, 4 H), 1.641 (s, 2 H) ( $\text{CH}_2$ ). Only some of the peaks for the *cis* trimer and both dimers could be positively identified because of low dimer concentration and the presence of small, concentration-independent peaks attributed to minor unidentified impurities [0.124 (s, *trans* dimer), 0.146 (s, *cis* dimer), 0.155 (s, *cis* dimer), 0.176, 0.201, 0.239, 0.285 ( $\text{SiMe}_3$ ); 0.628, 0.588, 0.470 ( $\text{GaMeCl}$ ); 1.719 (s, *cis* trimer), 1.364 (s, *cis* trimer) ( $\text{CH}_2$ )]. The ratios of dimer to trimer [tube A, 0.091:1; B, 0.041:1; C, 0.025:1], and *cis* to *trans* dimer (1:1) were obtained from the  $\text{Me}_3\text{Si}$  lines by using integrals and intensities respectively; the *cis* to *trans* trimer ratio (0.07:1, all concentrations) was obtained from  $\text{CH}_2$  intensities. The identities of dimer and trimer were confirmed by the slope (1.47  $\pm$  0.01) of the plot of the natural logarithm of the integral fractions of the dimer peaks times the total concentration (in monomeric units) vs. the same for the trimer peaks.  $\Delta G$  for the dimer-trimer equilibrium was calculated from the mean equilibrium constant,  $(1.75 \times 10^5) \pm (1.6 \times 10^4)$ , ( $K = [\text{T}]^2/[\text{D}]^3$ ); 9.4<sup>6</sup> was used as the molarity of toluene- $d_8$ .

$\{[(\text{Me}_3\text{SiCH}_2)_2\text{AsGaClPh}]\}_2$  (5).  $\text{PhGaCl}_2$  (1.02 g, 4.68 mmol) in benzene and 1 (1.54 g, 4.77 mmol) in pentane were combined and the clear solution was allowed to stand at room temperature for 1 day. The volatiles were removed in vacuo, leaving a foamy solid which was crystallized from hot ligroin. After several days, the mother liquor was removed, and the white solid was dried in vacuo (1.3 g, 65%), mp 133–138 °C. Anal. Calcd (Found) for  $\text{C}_{14}\text{H}_{27}\text{Si}_2\text{AsGaCl}$ : C, 38.96 (38.96); H, 6.31 (6.32). Mol wt (cryoscopic, 0.499 g in 15.27 g of benzene) 431.65n (1009  $\pm$  69,  $n = 2.34$ ). NMR:  $^{13}\text{C}\{^1\text{H}\}$  ( $\text{C}_6\text{D}_6$ , 75.429 MHz)  $\delta$  143.94, 137.20, 137.11, 137.0, 136.88, 136.60, 136.30, 129.33, 129.26, 128.60, 128.38 (m, Ph), 7.36, 7.06, 6.98, 6.81, 6.39 (m,  $\text{CH}_2$ ), 2.12, 1.79, 1.70, 1.62, 1.47, 1.44, 1.35, 1.13, 0.89 (m,  $\text{SiMe}_3$ ).

**NMR Equilibrium Study of 5.** Sealed NMR tubes containing three different concentrations of 5 in toluene- $d_8$  [(A) 0.0114/n M, (B) 0.0541/n M, (C) 0.158/n M] were kept at 25.0 °C for 6 days. The predominant *trans* trimer was identified by its distinctive pattern, dimer and *cis* trimer peaks were identified by observing their variation with concentration. NMR ( $^1\text{H}$ , 300 MHz): *trans* trimer  $\delta$  -0.074 (9 H), -0.056 (18 H), 0.047 (18 H), 0.132 (9 H) (s,  $\text{SiMe}_3$ ), 1.628 (s, 2 H), 1.579 and 1.607  $^2J_{\text{HH}} = 14.0$  Hz (AB pattern, 4 H), 1.852 and 1.900  $^2J_{\text{HH}} = 14.2$  Hz (AB pattern, 4 H), 1.673 (s, 2 H) ( $\text{CH}_2$ ), 8.05 (m, 4 H), 7.99 (m, 2 H)  $^3J_{\text{HH}} = 7.9$  Hz,  $^4J_{\text{HH}} = 1.3$  Hz (ortho H), 7.31–7.23 (m, 6 H), 7.19–7.13 (m, 3 H) (meta, para Ph); *cis* trimer -0.113 (27 H), 0.324 (27 H) (s,  $\text{SiMe}_3$ ), 1.828 (6 H), 1.429 (6 H) (s,  $\text{CH}_2$ ); dimer 0.034 (s,  $\text{SiMe}_3$ ), 1.454 (*trans*), 1.657 (*cis*), 1.787 (*cis*) (s,  $\text{CH}_2$ ); other noticeable Ph peaks overlap with *trans* trimer multiplet at 7.16, dimer may overlap peak at 0.047, and small unidentified peaks are present.

The ratios of dimer to trimer [tube (A) 0.26:1, (B) 0.15:1, (C) 0.11:1] and *cis* to *trans* dimer (1:1, all concentrations) were obtained from the integrals of their  $\text{CH}_2$  peaks; the *cis* to *trans* trimer

(5) (a) Schmidbaur, H.; Findeiss, W. *Chem. Ber.* 1966, 99, 2187. (b) Perkins, P. G.; Twentyman, M. E. *J. Chem. Soc.* 1965, 1038.

(6) *Langes Handbook of Chemistry*, 13th ed.; McGraw-Hill: New York, 1985; p 7-646.

ratio (0.08:1, all concentrations) was obtained from  $\text{Me}_3\text{Si}$  intensities. A  $\ln/\ln$  plot similar to that for 4 (slope =  $1.49 \pm 0.02$ ) confirmed the dimer-trimer equilibrium [mean  $K = (5.1 \times 10^4) \pm (3 \times 10^3)$ ].

**Crystallographic Measurements.** Preliminary unit-cell parameters and space group information were obtained from oscillation and Weissenberg photographs. Intensity data ( $h, \pm k, \pm l$ ) were recorded on an Enraf-Nonius CAD-4 diffractometer (Cu  $K\alpha$  radiation, incident-beam graphite monochromator;  $\omega$ - $2\theta$  scans,  $\theta_{\text{max}} = 67^\circ$ ). From a total of 5501 independent reflections after averaging equivalent forms, those 4687 with  $I > 3.0\sigma(I)$  were retained for the structure analysis and corrected for the usual Lorentz and polarization effects. An empirical absorption correction, based on the  $\phi$  dependence of the intensities of four reflections with  $\chi$  ca.  $90^\circ$  ( $T_{\text{max}}:T_{\text{min}} = 1.0:0.46$ ), was also applied to these data. Refined unit-cell parameters were derived from the diffractometer setting angles for 25 reflections ( $57^\circ < \theta < 67^\circ$ ) widely separated in reciprocal space.

**Structure Analysis.** The crystal structure was solved by the heavy-atom approach. Approximate coordinates for the As, Br, and Ga atoms were derived from a Patterson map, and those for the remaining non-hydrogen atoms were obtained from subsequent  $F_o$  and difference Fourier syntheses. Full-matrix least-squares adjustment of non-hydrogen atom positional and anisotropic thermal parameters, with hydrogen atoms, save those on C(43) and C(44) which have very large vibrational amplitudes, included at their calculated positions in the later iterations, converged to  $R = 0.056$  ( $R_w = 0.082$ ).<sup>7,8</sup> For the structure-factor calculations, neutral atom scattering factors and their anomalous dispersion corrections were taken from ref 9. In the least-squares iterations,  $\sum w\Delta^2$  [ $w = 1/\sigma^2(|F_o|)$ ;  $\Delta = (|F_o| - |F_c|)$ ] was minimized.

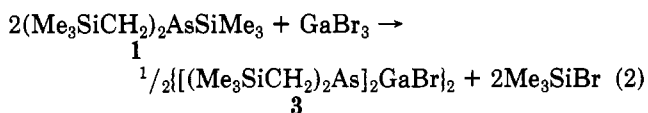
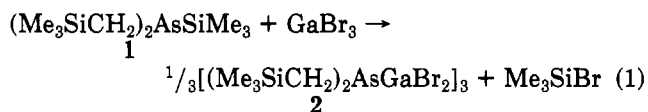
**Dynamic NMR Studies.**  $^{13}\text{C}\{^1\text{H}\}$  (75.429 MHz) spectra of 3 were obtained at the temperatures  $-7.5, 2.5, 21, 31, 36, 41, 46, 51, 57, 67, 75, 76, 82,$  and  $87^\circ\text{C}$  by using a sealed 5-mm NMR tube containing an approximately 0.034 M solution of 3 in  $\text{C}_6\text{D}_5\text{CD}_3$ . Typical conditions for  $^{13}\text{C}\{^1\text{H}\}$  observation were a flip angle of  $48^\circ$ , 2.3-s repetition rate, 2643-Hz spectral width, 512–2048 transients, no line broadening, and 32 K transform. The temperature controller on the Varian XL-300 was calibrated with a tube of freshly distilled ethylene glycol. The separation (Hz) between the trans  $\text{Me}_3\text{Si}$  peak was plotted vs. temperature ( $^\circ\text{C}$ ) for the spectra taken up to  $46^\circ\text{C}$ , after which the exchange process begins to have an appreciable effect on peak separation. The slope for the lowest temperatures ( $-7.5, 2.5,$  and  $21^\circ\text{C}$ ; eq A,  $\Delta\nu = 0.0826T + 85.81$ ) was almost twice the slope for the higher temperature range ( $21$ – $46^\circ\text{C}$ ; eq B,  $\Delta\nu = 0.0435T + 86.71$ ). The  $\text{Me}_3\text{Si}$  region of the  $^{13}\text{C}\{^1\text{H}\}$  spectra ( $21$ – $87^\circ\text{C}$ ) was simulated with the modified DNMR3<sup>10a</sup> program, using two sites and four configurations (two cis and two trans). The half-height line widths (0.7 Hz for both the cis and trans isomers) of the  $\text{Me}_3\text{Si}$  peaks at  $2.5^\circ\text{C}$  were used for minimum  $T_2$  values (0.5 s). The populations were calculated from the trans/cis ratio at  $2.5^\circ\text{C}$  using the equation  $\ln(P_T/P_C) = -\Delta G_{T/C}/RT$ .<sup>10b</sup> Simulations were visually compared to the recorded spectra with a lightbox. A preliminary simulation, where the cis peaks were ignored (a two-site exchange), was performed and the rate constants ( $k$ , temp) (0.7, 21), (3, 31), (6, 36), (11, 41), (17, 46), (23, 51), (36, 57), (80, 67), (157, 75), (175, 76), (250, 82), and (345  $\text{s}^{-1}$ ,  $87^\circ\text{C}$ ) were obtained. Then, with the cis peaks included, the trans-cis rate constant ( $k_1$ ) [assumption:  $k_1 = k_5$ ] was varied and the trans-trans rate constant ( $k_4$ ) was decreased until the best fit was obtained between the simulated and recorded spectra. The judgement of best fit for the  $21$ – $57^\circ\text{C}$  spectra was based upon the height discrepancy between the coalescing cis-trans pairs, the overall line width, and the line shape near the base line where the effect of the cis peaks is greatest. The rate

constants for the spectra taken at  $67, 75,$  and  $76^\circ\text{C}$  were determined by varying  $k_1$  and  $k_4$  and identifying the simulations that most closely approximated the line widths and the heights of the depressions between the coalescing peaks. The rate constants ( $k_1, k_4$ , temp) (0.2, 0.7, 21), (0.7, 2.3, 31), (1.0, 4.0, 36), (2.1, 7.0, 41), (3.0, 12, 46), (4.0, 18, 51), (5.0, 29, 57), (15, 65, 67), (25, 130, 75), and (30  $\text{s}^{-1}$ , 145  $\text{s}^{-1}$ ,  $76^\circ\text{C}$ ) were obtained. Covariance between  $k_1$  and  $k_4$  reduced the certainty in the last three measurements, and prevented determination of  $k_1$  and  $k_4$  for the temperatures above coalescence.

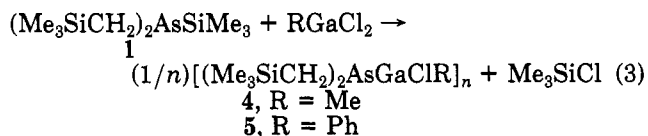
A least-squares linear regression analysis of  $\ln(k/T)$  vs.  $(1/T)$  yielded a slope ( $m$ ) and an intercept ( $b$ ) (for  $k_1$   $m = -8751 \pm 338$ ,  $b = 22.63 \pm 1.05$ ; for  $k_4$   $m = -9397 \pm 168$ ,  $b = 26.04 \pm 0.52$ ). The equations<sup>10b</sup>  $\Delta H^\ddagger = -mR$ ,  $\Delta S^\ddagger = R(b - 23.76)$ , were used to obtain  $\Delta H^\ddagger$  and  $\Delta S^\ddagger$ . Reported errors are standard deviations from least squares only.

## Results and Discussion

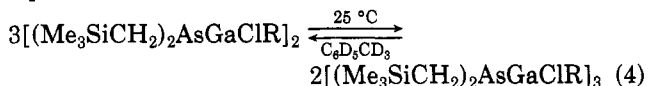
**Trimethylsilyl Cleavage Reactions.** Gallium tribromide, like  $\text{GaCl}_3$ ,<sup>1a</sup> reacts with  $(\text{Me}_3\text{SiCH}_2)_2\text{AsSiMe}_3$  (1) at room temperature in hydrocarbon solvents



The easily crystallized products, trimer 2 and dimer 3 were shown to have the same degree of oligomerization in solution as their chloro analogues,<sup>1a</sup>  $[(\text{Me}_3\text{SiCH}_2)_2\text{AsGaCl}_2]_3$  and  $\{[(\text{Me}_3\text{SiCH}_2)_2\text{As}]_2\text{GaCl}\}_2$ , by cryoscopic molecular weight determinations. The NMR spectrum of 2 shows a single species, consistent with its formulation as a trimer. The spectrum of 3 is discussed in a later section. Compound 2 was isolated in an excellent (87%) yield, whereas the 30% yield of 3 possibly reflects its appreciable solubility in the crystallization solvent, ligroin. The silylarsine, 1, also reacts readily with organogallium dichlorides,  $\text{RGaCl}_2$ , in a 1:1 ratio



The cryoscopic molecular weights of the white, crystalline products 4 and 5 were obtained in cyclohexane and benzene, respectively; both have a degree of association between 2 and 3. The concentration dependence of the NMR spectra confirms the presence of dimer-trimer equilibria



$$4, \text{R} = \text{Me}, \Delta G = -8.5 \pm 0.1 \text{ kcal/mol}$$

$$5, \text{R} = \text{Ph}, \Delta G = -6.4 \pm 0.1 \text{ kcal/mol}$$

The predominant species for both compounds are the trans trimers (4,  $\Delta G_{\text{cis-trans}} = -1.6 \pm 0.2 \text{ kcal/mol}$ ; 5,  $\Delta G_{\text{cis-trans}} = -1.5 \pm 0.1 \text{ kcal/mol}$ ); for the dimers the cis-trans equilibrium constants equal 1 within experimental error.

**Crystal Structure of  $\{[(\text{Me}_3\text{SiCH}_2)_2\text{As}]_2\text{GaBr}\}_2$  (3).** An ORTEP drawing of 3 is shown in Figure 1. Crystal data are presented in Table I, atomic coordinates for the non-hydrogen atoms in Table II, and selected bond lengths and angles in Table III.

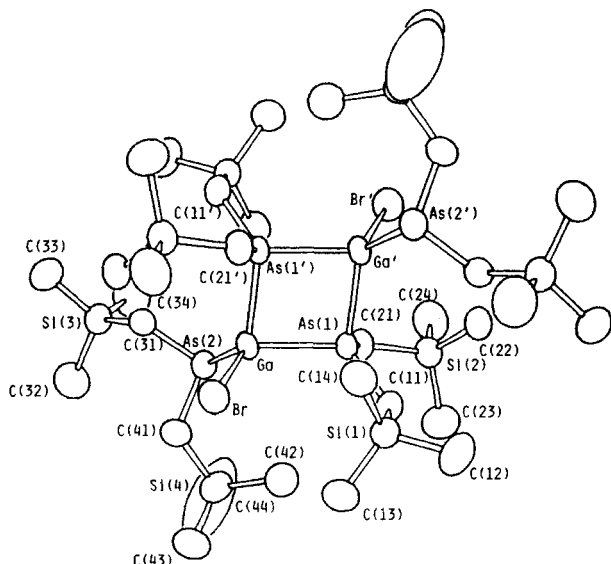
In the solid state, with one molecule per unit cell in space group  $P\bar{1}$ , dimer 3 is required to lie on a crystallographic center of symmetry and comprise a planar  $(\text{Ga-As})_2$  ring

(7) All crystallographic calculations were performed on a PDP11/44 computer by the use of the Enraf-Nonius SDP suite of programs.

(8)  $R = \sum(|F_o| - |F_c|) / \sum|F_o|$ ;  $R_w = [\sum w(|F_o| - |F_c|)^2 / \sum w|F_o|^2]^{1/2}$ .

(9) *International Tables for X-Ray Crystallography*; Kynoch: Birmingham, England, 1974; Vol. IV.

(10) (a) Binsch, G.; Kleier, D. A. *The Computation of Exchange Broadened NMR Spectra*, Program 165; Quantum Chemistry Program Exchange, Indiana University: Bloomington, IN, 1970; revised by Bushweller, C. H.; Bhat, G.; Letendre, L. J.; Brunelle, J. A.; Bilofsky, H. S.; Ruben, H.; Templeton, D. H.; Zalkin, A. *J. Am. Chem. Soc.* **1975**, *97*, 65, and by Caves, T., North Carolina State University. (b) Sandstrom, J. *Dynamic NMR Spectroscopy*; Academic: London, England, 1982.

Figure 1. ORTEP drawing of  $[(\text{Me}_3\text{SiCH}_2)_2\text{As}]_2\text{GaBr}_2$  (3).Table I. Crystal Data for  $[(\text{Me}_3\text{SiCH}_2)_2\text{As}]_2\text{GaBr}_2$ 

formula	$\text{C}_{32}\text{H}_{88}\text{As}_4\text{Br}_2\text{Ga}_2\text{Si}_8$
fw	1296.69
sample	sealed under $\text{N}_2$ in a 0.5-mm glass capillary
crystal size, mm	$0.42 \times 0.42 \times 0.22$
crystal habit	plates
crystal system	triclinic
space group	$P\bar{1}$
temperature, $^\circ\text{C}$	21
$a$ , $\text{\AA}$	11.892 (2)
$b$ , $\text{\AA}$	12.492 (2)
$c$ , $\text{\AA}$	11.515 (1)
$\alpha$ , deg	98.24 (1)
$\beta$ , deg	113.57 (1)
$\gamma$ , deg	84.21 (1)
$Z$	1
$d_{\text{calc}}$ , $\text{g/cm}^3$	1.389
$V$ , $\text{\AA}^3$	1549.9
radiation, $\text{\AA}$	$\text{Cu K}\alpha$ , $\lambda = 1.5418$
$\mu$ ( $\text{cm}^{-1}$ ), absorption coefficient ( $\text{Cu K}\alpha$ )	66.5

with trans-related  $(\text{Me}_3\text{SiCH}_2)_2\text{As}$  substituents at Ga. Four other structures containing similar rings have been reported previously, viz.,  $[(\text{Me}_3\text{SiCH}_2)_2\text{AsGaPh}_2]_2$  (6),<sup>1d</sup>  $[(\text{Me}_3\text{SiCH}_2)_2\text{As}]_3\text{Ga}_2$  (7),<sup>4g</sup> and  $[(t\text{-Bu}_2\text{AsGaR}_2)_2]$  ( $\text{R} = \text{Me}$  (8) and  $\text{R} = n\text{-Bu}$  (9)).<sup>3</sup> Whereas the centrosymmetric rings in 6 and 8 are, as with 3, crystallographically constrained to be planar, and that in 9 is almost planar, the ring in 7 is butterfly shaped. Bond lengths in the planar  $(\text{Ga-As})_2$  ring of 3 [ $\text{Ga-As}(1) = 2.513$  (1)  $\text{\AA}$ ,  $\text{Ga-As}(1') = 2.521$  (1)  $\text{\AA}$ ] are similar to those in the mono(arsino)gallane 6 [2.518 (1)  $\text{\AA}$  and 2.531 (1)  $\text{\AA}$ ] but are shorter than the corresponding distances in the more sterically crowded 8 and 9 [range 2.541 (1)–2.558 (1)  $\text{\AA}$ ] and highly strained 7 [2.540 (1)–2.581 (1)  $\text{\AA}$ ]. Endocyclic bond angles at Ga [84.37 (1) $^\circ$ ] and As [95.63 (2) $^\circ$ ] in 3 lie within the fairly narrow ranges [83.58 (4)–85.02 (2) $^\circ$ ] and [94.57 (4)–96.02 (4) $^\circ$ ], respectively, found in 6, 7, 8, 9, and thus these angles appear in general to be relatively insensitive to the nature of the ring substituents.

The bond length from Ga to the exocyclic three-coordinate arsenic, As(2), at 2.437 (1)  $\text{\AA}$ , is like corresponding distances in 7 [2.470 (1)–2.478 (2)  $\text{\AA}$ ], significantly shorter than the ring bonds. Moreover, it is also smaller than the shortest Ga–As distance of 2.470 (1)  $\text{\AA}$  in  $(\text{Me}_2\text{As})_3\text{Ga}$ ,<sup>1e</sup> where some bond length extension may be present due to severe steric overcrowding, and represents the shortest distance yet encountered between these centers in an organogallium–arsenic compound.

Table II. Non-Hydrogen Atom Fractional Coordinates ( $\times 10^4$ ), with Estimated Standard Deviations in Parentheses

atom	x	y	z
Ga	1031.3 (5)	-1108.6 (5)	-350.9 (5)
As(1)	-1231.1 (4)	-616.5 (4)	-1137.8 (4)
As(2)	1751.8 (5)	-2870.0 (5)	422.3 (6)
Br	1832.0 (5)	-746.0 (7)	-1837.2 (5)
Si(1)	-1926 (1)	66 (1)	-4067 (1)
Si(2)	-3606 (1)	-1736 (1)	-1038 (1)
Si(3)	4385 (1)	-3444 (1)	2686 (2)
Si(4)	1031 (2)	-4316 (2)	-2328 (3)
C(11)	-2265 (4)	-707 (5)	-2966 (5)
C(12)	-3420 (7)	546 (7)	-5229 (7)
C(13)	-1176 (5)	-908 (6)	-4947 (6)
C(14)	-976 (5)	1252 (5)	-3215 (6)
C(21)	-1878 (4)	-1680 (4)	-503 (4)
C(22)	-4418 (5)	-386 (5)	-1285 (5)
C(23)	-4194 (7)	-2677 (6)	-2580 (8)
C(24)	-3872 (6)	-2288 (6)	245 (7)
C(31)	3401 (5)	-2392 (4)	1667 (5)
C(32)	4800 (7)	-4621 (5)	1707 (8)
C(33)	5829 (7)	-2817 (7)	3839 (8)
C(34)	3572 (8)	-3913 (7)	3594 (8)
C(41)	2228 (7)	-3560 (6)	-988 (7)
C(42)	-430 (8)	-3561 (8)	-2874 (9)
C(43)	1542 (12)	-4466 (20)	-3705 (11)
C(44)	965 (19)	-5586 (11)	-2011 (30)

Table III. Bond Lengths ( $\text{\AA}$ ) and Bond Angles (deg), with Estimated Standard Deviations in Parentheses

(a) Bond Lengths			
Ga–As(1)	2.513 (1)	Si(2)–C(21)	1.900 (5)
Ga–As(2)	2.437 (1)	Si(2)–C(22)	1.857 (6)
Ga–Br	2.378 (1)	Si(2)–C(23)	1.897 (7)
Ga–As(1')	2.521 (1)	Si(2)–C(24)	1.862 (9)
As(1)–C(11)	1.961 (4)	Si(3)–C(31)	1.873 (5)
As(1)–C(21)	1.956 (6)	Si(3)–C(32)	1.871 (8)
As(2)–C(31)	2.000 (4)	Si(3)–C(33)	1.864 (7)
As(2)–C(41)	1.984 (8)	Si(3)–C(34)	1.863 (11)
Si(1)–C(11)	1.882 (7)	Si(4)–C(41)	1.843 (7)
Si(1)–C(12)	1.849 (7)	Si(4)–C(42)	1.808 (9)
Si(1)–C(13)	1.858 (7)	Si(4)–C(43)	1.892 (16)
Si(1)–C(14)	1.862 (6)	Si(4)–C(44)	1.694 (19)
(b) Bond Angles			
As(1)–Ga–As(2)	118.37 (3)	C(21)–Si(2)–C(23)	107.9 (3)
As(1)–Ga–Br	110.41 (3)	C(21)–Si(2)–C(24)	106.8 (3)
As(1)–Ga–As(1')	84.37 (2)	C(22)–Si(2)–C(23)	109.8 (3)
As(2)–Ga–Br	112.60 (3)	C(22)–Si(2)–C(24)	108.8 (3)
As(2)–Ga–As(1')	112.31 (3)	C(23)–Si(2)–C(24)	110.6 (4)
Br–Ga–As(1')	105.34 (3)	C(31)–Si(3)–C(32)	111.4 (3)
Ga–As(1)–C(11)	121.3 (2)	C(31)–Si(3)–C(33)	108.3 (3)
Ga–As(1)–C(21)	103.8 (1)	C(31)–Si(3)–C(34)	109.8 (3)
Ga–As(1)–Ga'	95.63 (2)	C(32)–Si(3)–C(33)	108.4 (4)
C(11)–As(1)–C(21)	104.3 (2)	C(32)–Si(3)–C(34)	110.1 (4)
C(11)–As(1)–Ga'	123.0 (2)	C(33)–Si(3)–C(34)	108.8 (4)
C(21)–As(1)–Ga'	106.9 (2)	C(41)–Si(4)–C(42)	112.5 (4)
Ga–As(2)–C(31)	95.2 (2)	C(41)–Si(4)–C(43)	105.7 (6)
Ga–As(2)–C(41)	98.2 (2)	C(41)–Si(4)–C(44)	111.4 (9)
C(31)–As(2)–C(41)	98.7 (3)	C(42)–Si(4)–C(43)	105.2 (6)
C(11)–Si(1)–C(12)	107.0 (3)	C(42)–Si(4)–C(44)	114.6 (8)
C(11)–Si(1)–C(13)	107.3 (3)	C(43)–Si(4)–C(44)	106.6 (14)
C(11)–Si(1)–C(14)	112.8 (3)	As(1)–C(11)–Si(1)	121.5 (3)
C(12)–Si(1)–C(13)	108.2 (3)	As(1)–C(21)–Si(2)	119.1 (2)
C(12)–Si(1)–C(14)	109.1 (3)	As(2)–C(31)–Si(3)	115.0 (3)
C(13)–Si(1)–C(14)	112.1 (3)	As(2)–C(41)–Si(4)	115.9 (4)
C(21)–Si(2)–C(22)	112.9 (3)		

Exocyclic bond angles at Ga reflect differences in the steric demands of the Br and bulky  $(\text{CH}_2)_2\text{SiMe}_3$  ring substituents. The As(1)–Ga–As(2) and As(1')–Ga–As(2) angles at 118.37 (3) $^\circ$  and 121.31 (3) $^\circ$ , respectively, are both significantly greater than any of the As–Ga–Br angles [112.60 (3) $^\circ$ , 110.4 (3) $^\circ$ , and 105.34 (3) $^\circ$ ] the largest of which also involves As(2). Likewise, exocyclic angles at As range widely from 104.3 (2) $^\circ$  to 123.0 (2) $^\circ$ , with the largest, Ga–As(1')–C(11'), involving the carbon atom C(11'), which lies cis to As(2) [As(2)–Ga–As(1')–C(11') dihedral angle = 13.2 $^\circ$ ]. At three-coordinate As(2), bond angles

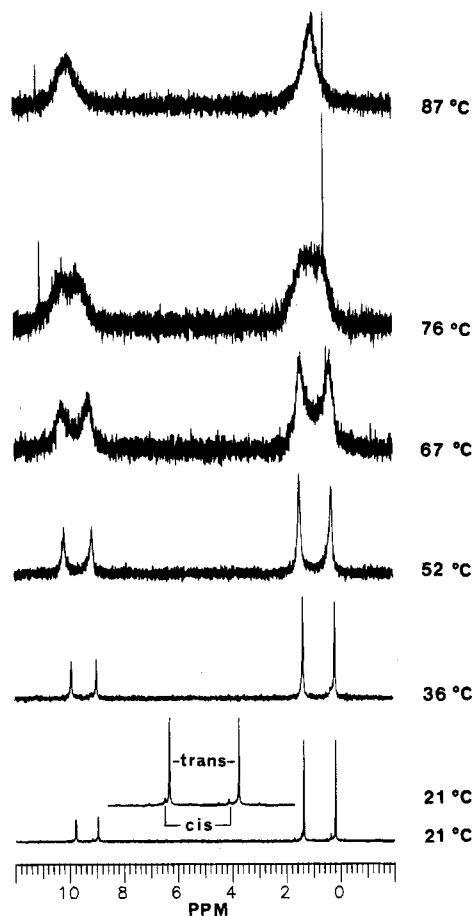


**Figure 2.**  $^{13}\text{C}\{^1\text{H}\}$  NMR spectra of  $[(\text{Me}_3\text{SiCH}_2)_2\text{As}]_2\text{GaBr}_2$  (3); insert is the expanded  $\text{Me}_3\text{Si}$  region of the 21 °C spectrum.

range from 95.2 (2)° to 98.2 (3)°, mean 97.4°, and, accordingly, the geometry at this center is clearly pyramidal.<sup>11</sup> The As–C–Si bond angles vary depending on the nature of the coordination of the As atom bearing the  $-\text{CH}_2\text{SiMe}_3$  groups. Thus, when As is four-coordinate, the mean bond angle is 120.3°, whereas with three-coordinate As, the corresponding value is reduced to 115.5°.

**NMR Analysis of  $[(\text{Me}_3\text{SiCH}_2)_2\text{As}]_2\text{GaBr}_2$  (3).** The  $^{13}\text{C}\{^1\text{H}\}$  NMR spectra of 3 in toluene- $d_6$  are reproduced in Figure 2. These spectra show the presence of both cis and trans isomers, with the trans being the predominant species. The trans/cis population ratio was determined from the intensities of the  $\text{Me}_3\text{Si}$  peaks to be 10.2 at 2.5 °C. Neglecting any difference in the NOE between cis and trans peaks, this corresponds to a  $\Delta G$  of 1.3 kcal/mol for the trans–cis equilibrium.

On the basis of the  $^{13}\text{C}\{^1\text{H}\}$  chemical shifts of  $[(\text{Me}_3\text{SiCH}_2)_2\text{As}]_3\text{Ga}_2$  (7),<sup>16,12</sup> where the endocyclic and exocyclic  $(\text{Me}_3\text{SiCH}_2)_2\text{As}$  groups are unambiguously identified from relative intensities, the downfield peaks of the  $\text{Me}_3\text{Si}$  region ( $\delta$  1.42 and 1.35) and the  $\text{CH}_2$  region of 3 ( $\delta$  9.77, 9.69, and 11.13) are assigned to the endocyclic  $(\text{Me}_3\text{SiCH}_2)_2\text{As}$  groups. This assignment is given further weight by the  $^{13}\text{C}\{^1\text{H}\}$  spectra of other  $[(\text{Me}_3\text{SiCH}_2)_2\text{AsGaR}_2]_n$  compounds,<sup>13</sup> the pattern of three cis- $\text{CH}_2$  peaks, and the slight extra broadening of the cis peak at  $\delta$  1.42 in the 21 °C spectrum. The two  $\text{Me}_3\text{SiCH}_2$

(11) For examples of bond angles around three-coordinate arsenic see (a) Sobolev, A. N.; Belsky, V. K. *J. Organomet. Chem.* 1981, 214, 41. (b) Hedberg, K.; Hughes, E. W.; Waser, J. *Acta Crystallogr.* 1961, 14, 369. (c) Trotter, J. *Can. J. Chem.* 1962, 40, 1590.

(12)  $[(\text{Me}_3\text{SiCH}_2)_2\text{As}]_3\text{Ga}_2$  has two exocyclic arsenic atoms for each endocyclic arsenic atom. Therefore the  $^{13}\text{C}\{^1\text{H}\}$  peaks are readily identified.  $^{13}\text{C}\{^1\text{H}\}$  ( $\text{C}_6\text{D}_6$ , 75.429 MHz):  $\delta$  0.98 (exo- $\text{SiMe}_3$ ), 2.02 (endo- $\text{SiMe}_3$ ), 6.69 (exo- $\text{CH}_2$ ), 10.59 (endo- $\text{CH}_2$ ).

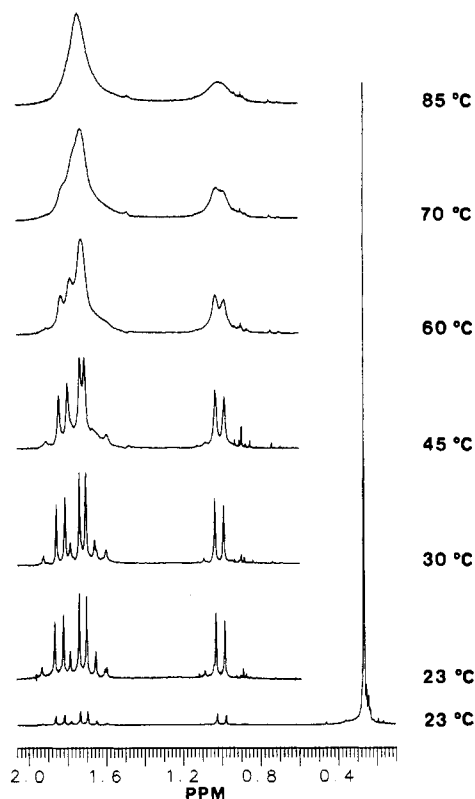


**Figure 3.**  $^1\text{H}$  NMR spectra of  $[(\text{Me}_3\text{SiCH}_2)_2\text{As}]_2\text{GaBr}_2$  (3).

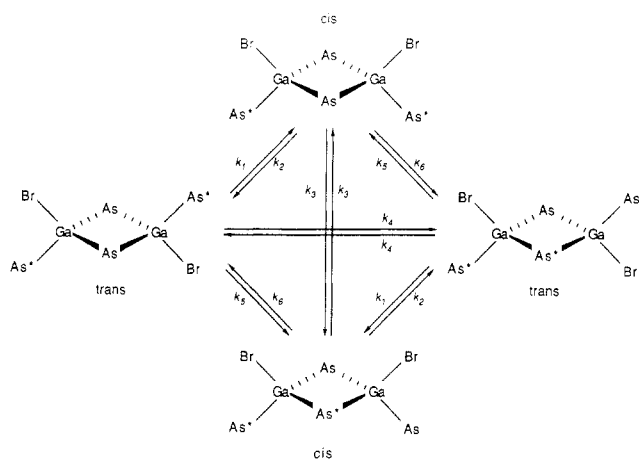
groups on the endocyclic arsenic in the cis isomer are magnetically inequivalent, and this peak must in fact be two overlapping resonances. Selective broadening of one cis peak cannot be explained by the exchange of  $(\text{Me}_3\text{SiCH}_2)_2\text{As}$  groups.

The  $^1\text{H}$  NMR spectra of 3 in benzene- $d_6$  are reproduced in Figure 3 and are fairly similar to the chloro analogue,<sup>1a</sup> the main difference being the more prominent AB pattern for the endocyclic trans- $\text{CH}_2$  protons in 3.<sup>14</sup>

When the temperature is raised from 2.5 to 87 °C, the  $^{13}\text{C}\{^1\text{H}\}$   $\text{Me}_3\text{Si}$  resonances of 3 first broaden and the cis and trans peaks start to merge. At 41 °C only two  $\text{Me}_3\text{Si}$  peaks are observable. Above 57 °C the  $\text{Me}_3\text{Si}$  peaks start to merge, coalescing at 76 °C. By 87 °C the single broad peak has sharpened considerably. The  $^{13}\text{C}\{^1\text{H}\}$   $\text{CH}_2$  peaks broaden in a similar manner as the temperature is raised and coalesce between 76 and 82 °C. The proton spectra show a behavior similar to the chloro analogue as the temperature is increased.<sup>1a</sup> The proton  $\text{CH}_2$  peaks broaden, then finally merge into two broad humps at 85 °C. The temperature was not increased sufficiently to

(13) The  $^{13}\text{C}$   $\text{SiMe}_3$  shifts of  $[(\text{Me}_3\text{SiCH}_2)_2\text{AsGaMe}_2]_2$  (1.5, 0.75),  $[(\text{Me}_3\text{SiCH}_2)_2\text{AsGaPh}_2]$  (0.9),  $[(\text{Me}_3\text{SiCH}_2)_2\text{AsGaCl}_2]$  (1.2), and compound 2 ( $\delta$  1.73) are all greater than  $\delta$  0.7, while the  $^{13}\text{C}\{^1\text{H}\}$   $\text{Me}_3\text{Si}$  shifts of compounds with tricoordinate arsenic,  $(\text{Me}_3\text{SiCH}_2)_2\text{AsX}$ , are usually less than  $\delta$  0.7; X = Cl, 0.4, X = H, -0.5, X = As( $\text{Me}_3\text{SiCH}_2$ ), 0.4, and X =  $\text{Me}_3\text{SiCH}_2$ , 0.1.

(14) We have previously reported that the endo- $\text{CH}_2\text{As}$  proton resonance of trans- $[(\text{Me}_3\text{SiCH}_2)_2\text{As}]_2\text{GaCl}_2$  is a singlet. When its spectrum was examined more closely following the preparation of 3, it was evident that this resonance is in fact an AB pattern. Other minor peaks in the  $^1\text{H}$  spectrum of the chloro analogue, which were previously not identified, are now assigned to its cis isomer. For  $[(\text{Me}_3\text{SiCH}_2)_2\text{As}]_2\text{GaCl}_2$ ,  $^1\text{H}$  NMR ( $^1\text{H}$ , 299.943 MHz): trans, ( $\text{C}_6\text{D}_6$ ) 0.27, 0.26 (s,  $\text{Me}_3\text{Si}$ ), 1.68 (endo- $\text{CH}_2\text{As}$ , AB pattern with nearly coincident central peaks; from the intensity ratio of outer peak to the central peak (38), the two resonances are calculated to be 0.75 Hz or ca.  $\delta$  0.003 apart;  $^2J_{\text{HH}} = 13.5$  Hz), 1.81 and 0.99,  $^2J_{\text{HH}} = 13.2$  Hz (AB pattern, exo- $\text{CH}_2\text{As}$ ), ( $\text{C}_6\text{D}_5\text{CD}_3$ ) 0.25, 0.27 (s,  $\text{SiMe}_3$ ), 1.65 (endo- $\text{CH}_2$ ), 0.94 and 1.76,  $^2J_{\text{HH}} = 13.5$  Hz (AB pattern, exo- $\text{CH}_2\text{As}$ ); cis, ( $\text{C}_6\text{D}_6$ ), 1.66 and 1.06,  $^2J_{\text{HH}} = 13.8$  Hz (AB pattern, exo- $\text{CH}_2\text{As}$ ), 1.57, 1.87 (s, endo- $\text{CH}_2\text{As}$ ),  $\text{Me}_3\text{Si}$  peaks hidden under trans; ( $\text{C}_6\text{D}_5\text{CD}_3$ ), 1.01 and 1.62,  $^2J_{\text{HH}} = 13.5$  Hz (exo- $\text{CH}_2\text{As}$ ), 1.56, 1.81 (s, endo- $\text{CH}_2\text{As}$ ),  $\text{Me}_3\text{Si}$  peaks hidden under trans.

**Scheme I. Rate Constants for Exchange between the Two Trans and Two Cis Sites in  $\{[(\text{Me}_3\text{SiCH}_2)_2\text{As}]_2\text{GaBr}\}_2$  (3)**

achieve complete coalescence. During heating, peaks corresponding to a decomposition product  $[(\text{Me}_3\text{SiCH}_2)_2\text{As}]_2$ <sup>1a,15</sup> grew. The exchange phenomenon is interpreted as interchange of the endocyclic and exocyclic arsino groups, a process similar to that reported for the chloro analogue, and which can be simulated by calculated spectra. The  $^{13}\text{C}\{^1\text{H}\}$   $\text{Me}_3\text{Si}$  peaks were chosen for the dynamic NMR study because utilizing the  $\text{CH}_2$  regions of the proton or carbon spectra would have been substantially more difficult.<sup>16</sup> Although reasonable approximations of the spectra can be obtained when the cis peaks are ignored, a proper simulation must take the cis peaks into account.

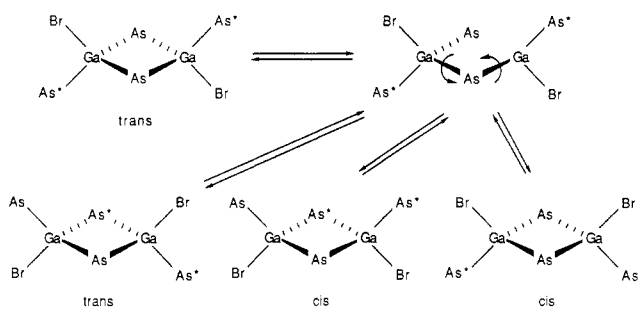
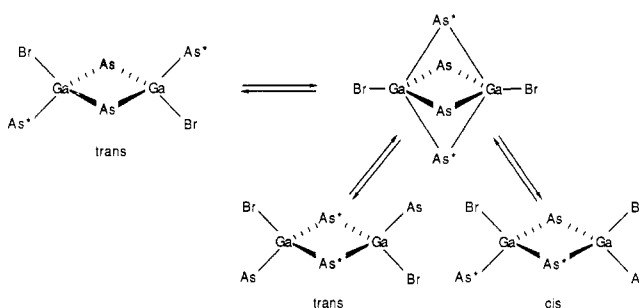
An exchange between four sites has six different rate constants (Scheme I). The simplifying assumption that both sets of cis–trans rate constants are equal (i.e.  $k_1 = k_5$ ,  $k_2 = k_6$ ) or that one set equals zero was made.<sup>17</sup> Also,  $k_2$  must equal the product of  $k_1$  and the trans/cis population ratio at each particular temperature. This leaves three independent rate constants,  $k_1$  (or  $k_5$ ),  $k_3$ , and  $k_4$  to be determined. The line widths of the large (trans) peaks are sensitive to both the cis–trans ( $k_1$ ,  $k_5$ ) and the trans–trans ( $k_4$ ) rate constants, but not to  $k_3$  which affects only the cis peaks.<sup>18</sup>

As the cis- and trans- $\text{Me}_3\text{Si}$  peaks begin to coalesce, a considerable discrepancy in peak height develops between the two coalescing cis–trans pairs. This is because the upfield-most trans peak is farther away from its cis companion than the other trans peak. For a given value of  $k_4$ , this height discrepancy is most sensitive to  $k_1$ .

A good fit could be obtained for the lower temperature spectra, where separate cis–trans pairs were still present (21–57 °C), and a simulation in which only  $k_1$  ( $k_1 = k_5$ ) and

**Table IV. Activation Parameters for Exchange in  $\{[(\text{Me}_3\text{SiCH}_2)_2\text{As}]_2\text{GaX}\}_2$ , X = Br, Cl**

compound	process	$\Delta H^\ddagger$ , kcal/mol	$\Delta S^\ddagger$ , cal/(mol K)	$\Delta G^\ddagger_{298}$ , kcal/mol
X = Br	trans–trans	$18.7 \pm 0.3$	$4.5 \pm 1.0$	17.3
3	( $k_4$ )			
3	trans–cis	$17.4 \pm 0.7$	$-2.2 \pm 2.1$	18.1
3	( $k_1$ , $k_5$ )			
3	trans–trans	$17.2 \pm 0.3$	$0.7 \pm 1.0$	17.0
	(cis ignored)			
X = Cl <sup>1a</sup>	trans–trans	$16.5 \pm 0.4$	$-1.55 \pm 1.3$	17.0
	(cis ignored)			

**Scheme II. Possible One-Bond Dissociative Mechanism for the Fluxional Processes in  $\{[(\text{Me}_3\text{SiCH}_2)_2\text{As}]_2\text{GaBr}\}_2$  (3)****Scheme III. Possible Associative Mechanism for the Fluxional Processes in  $\{[(\text{Me}_3\text{SiCH}_2)_2\text{As}]_2\text{GaBr}\}_2$  (3)**

$k_4$  were varied. Obtaining proper height discrepancy, line width, and line shape for both the cis and trans peaks, or both coalescing cis–trans pairs, did not require the use of  $k_3$ . As the temperature was increased, however, the separation between the cis–trans pairs had to be increased slightly in order to optimize the fit. The higher temperature spectra (>57 °C) could also be simulated by varying  $k_1$  and  $k_4$  alone, but the rate constants obtained were not as accurate. Among other things,<sup>19</sup> this inaccuracy is due to some covariance among the rate constants. The amount of covariance for the spectra taken at 67, 75, and 76 °C was small enough to allow a determination of  $k_1$  and  $k_4$  to be made, but these measurements, especially those of  $k_1$ , may possess considerable error. Unique simulations of the spectra above the coalescence temperature could not be made because the covariance between the rate constants became too great. However, a good simulation could be produced by making only slight adjustments to the values of  $k_1$  and  $k_4$  extrapolated from the results at lower temperatures.

Values of  $\Delta H^\ddagger$  and  $\Delta S^\ddagger$  (Table IV) were obtained from an Eyring plot and least-squares analysis of the data. Little mechanistic information about the exchange process

(15) All bis- and tris(arsino)gallanes prepared to date undergo a slow decomposition at room temperature to  $(\text{R}_2\text{As})_2$ . The decomposition rate increases with heating. The colored and the gallium-containing products of this decomposition have not been identified.

(16) The modified DNMR3 program<sup>9a</sup> can accept a maximum of four chemical configurations. Simulating the  $^{13}\text{C}\{^1\text{H}\}$   $\text{CH}_2$  region requires five, and the  $^1\text{H}$  case requires nine. Furthermore the signal to noise ratio for the cis- $\text{CH}_2$  carbon peaks in the recorded spectra were too low to be clearly seen at elevated temperatures.

(17) Simulations were attempted where either  $k_1$  and  $k_2$  or  $k_5$  and  $k_6$  were set to 0. The first case, with  $k_1$  and  $k_2 = 0$ , did not produce reasonable spectra. The second case ( $k_5$  and  $k_6 = 0$ ) produced better spectra, but still deviated from the experimental spectra more than the  $k_1 = k_5$  case. Note that in one of the proposed mechanisms (1-bond dissociation)  $k_1$  would be greater than  $k_5$ , but in all the other proposed mechanisms (one- or two-bond association and dissociation to monomers)  $k_1$  would equal  $k_5$ .

(18) When the cis and trans peaks coalesce,  $k_3$  does affect the total line shape. Still, moderately large changes in  $k_3$  affect the line shape to a small extent, and as the other rate constants increase the effect of  $k_3$  is even less pronounced. This makes the true values of  $k_3$  impossible to determine.

(19) Inaccuracy in rate constant determination arises from decomposition, poor base-line resolution, insufficient signal to noise ratio for broad peaks, and the assumptions made in the analysis, i.e.  $k_1 = k_5$ , the separation between cis and trans peaks remains constant, and that separation between the cis–trans pairs follows eq B.



can be obtained from these activation parameters. The small  $\Delta S^\ddagger$  indicates a unimolecular mechanism which may be dissociative or associative. One dissociative mechanism (Scheme II) involves the cleavage of a single Ga-As bond, rotation about the opposite (Ga-As) bond, and/or rotation around the adjacent (Ga-As) bond, and recombination. Reported values for the  $\Delta H$  of dissociation of  $\text{Me}_3\text{Ga}\cdot\text{AsR}_3$  adducts range from 8.2 to 14.6 kcal/mol.<sup>20</sup>

Exchange through an intermediate with five-coordinate gallium is another mechanistic possibility. One, or both exo-As atoms coordinates with the opposite Ga atom, and then one Ga-As bond to each five-coordinate gallium atom dissociates (Scheme III). Precedent for five-coordinate gallium exists.<sup>21</sup> One cannot distinguish between the

mechanisms with the data available.

**Acknowledgment.** The financial support for this work by the Office of Naval Research is gratefully acknowledged.

**Registry No.** 1, 101860-04-2; 2, 109997-38-8; *cis*-3, 109997-39-9; *trans*-3, 110044-17-2; *cis*-4 ( $n = 2$ ), 109997-40-2; *trans*-4 ( $n = 2$ ), 110044-51-4; *cis*-5 ( $n = 3$ ), 109997-41-3; *trans*-5 ( $n = 3$ ), 110044-18-3; GaBr<sub>3</sub>, 13450-88-9; MeGaCl<sub>2</sub>, 6917-74-4; PhGaCl<sub>2</sub>, 1073-46-7; Ga, 7440-55-3; As, 7440-38-2.

**Supplementary Material Available:** Tables of hydrogen atom coordinates, anisotropic temperature factors, and torsion angles (4 pages); a listing of observed and calculated structure amplitudes (32 pages). Ordering information is given on any current masthead page.

(20) (a) Coates, G. E. *J. Chem. Soc.* 1951, 2003. (b) Gribov, B. G.; Gusakov, G. M.; Kozyrkin, B. I.; Zorina, E. N. *Dokl. Akad. Nauk SSSR* 1973, 210(6), 1350. (c) Baev, A. K.; Gaidym, I. L. *Zh. Fiz. Khim.* 1975, 49, 976. (d) Tsvetkov, V. G.; Kozyrkin, B. I.; Fukin, K. K. Galivllina, R. *F. Zh. Ob. Khim.* 1977, 49(9), 2155.

(21) See for example: (a) Pattison, I.; Wade, K. *J. Chem. Soc. A* 1968, 2618. (b) Dymock, K.; Palenik, G. J. *J. Chem. Soc., Chem. Commun.* 1973, 884. (c) Rettig, S. J.; Storr, A.; Trotter, J. *Can. J. Chem.* 1976, 54, 1278. (e) McPhail, A. T.; Miller, R. W.; Pitt, C. G.; Gupta, G.; Srivastava, S. C. *J. Chem. Soc., Dalton Trans.* 1976, 1657.

## Preparation and Crystal Structures of (1,1'-Ruthenocenedithiolato-*S,S'*,*Ru*)(triphenylphosphine)- nickel(II) and (1,1'-Metalocenedioxalato-*O,O'*,*Fe*- (or *Ru*))(triphenylphosphine)palladium(II): The Metal (Fe or Ru)-Metal (Pd or Ni) Dative Bond

Sadatoshi Akabori,\* Takeshi Kumagai, and Toshio Shirahige

*Department of Chemistry, Faculty of Science, Toho University, Funabashi, Chiba 274, Japan*

Sadao Sato, Kayoko Kawazoe, and Chihiro Tamura

*Analytical and Metabolic Research Laboratories, Sankyo Co., Ltd., 1-2-58 Hiromachi, Shinagawa-ku,  
Tokyo 140, Japan*

Masaru Sato

*Chemical Analysis Center, Saitama University, Urawa, Saitama 338, Japan*

Received January 26, 1987

The reaction of 1,2,3-trithia[3](1,1')ruthenocenophane with  $\text{Ni}(\text{PPh}_3)_4$  in THF at room temperature gave  $[\text{Ru}(\eta^5\text{-C}_5\text{H}_4\text{S})_2]\text{NiPPh}_3$ , although  $[\text{Fe}(\eta^5\text{-C}_5\text{H}_4\text{S})_2]\text{NiPPh}_3$  could not be obtained in a similar reaction between  $\text{Ni}(\text{PPh}_3)_4$  and 1,2,3-trithia[3](1,1')ferrocenophane.  $[\text{Fe}(\eta^5\text{-C}_5\text{H}_4\text{O})_2]\text{PdPPh}_3$  and  $[\text{Ru}(\eta^5\text{-C}_5\text{H}_4\text{O})_2]\text{PdPPh}_3$  were obtained by the reaction of the disodium salt of the metallocenediols ( $M = \text{Fe}$  or  $\text{Ru}$ ) with  $\text{Pd}(\text{PPh}_3)_2\text{Cl}_2$  in 28% yield. Palladium complexes could not be obtained via analogous methods.  $[\text{Ru}(\eta^5\text{-C}_5\text{H}_4\text{S})_2]\text{NiPPh}_3 \cdot \frac{1}{2}\text{C}_6\text{H}_5\text{CH}_3$  crystallizes in the monoclinic space group  $C2/c$  with  $Z = 8$  and unit cell parameters  $a = 39.036$  (7) Å,  $b = 10.463$  (2) Å,  $c = 13.793$  (4) Å, and  $\beta = 102.03$  (2)°. The structure was refined to give  $R = 3.7\%$  using 3840 independent reflections with  $F_o \geq 2\sigma(F_o)$ .  $[\text{Ru}(\eta^5\text{-C}_5\text{H}_4\text{O})_2]\text{PdPPh}_3$  crystallizes in the monoclinic space group  $P2_1/n$  with  $Z = 4$  and unit cell parameters  $a = 11.022$  (6) Å,  $b = 14.872$  (10) Å,  $c = 14.454$  (5) Å, and  $\beta = 99.14$  (3)°. The structure was refined to  $R = 3.9\%$  using 3699 independent reflections with  $F_o \geq 2\sigma(F_o)$ . X-ray crystal data showed that  $[\text{Ru}(\eta^5\text{-C}_5\text{H}_4\text{O})_2]\text{PdPPh}_3$  and  $[\text{Fe}(\eta^5\text{-C}_5\text{H}_4\text{O})_2]\text{PdPPh}_3$  are isomorphous. The distances between the metal-metal and the large chemical shifts between the  $\alpha$ - and  $\beta$ -ring protons in the <sup>1</sup>H NMR spectra of their complexes provide for appreciable evidence of Ru-Pd (or Fe-Pd and Ru-Ni) dative bonding.

### Introduction

The coordination of the nonbonding d electrons ( $e_{2g}$  electrons) of the iron atom in the ferrocenophane nucleus to the vacant orbitals of another metal atom has been reported by Sano et al.<sup>1</sup> in [2](1,1')ferrocenophane-metal halide. However, Whitesides et al.,<sup>2</sup> McCulloch et al.<sup>3</sup> and

Butter et al.<sup>4</sup> reported no evidence of such kind of interaction between the iron atom and the platinum group metal atoms in compounds 1 and 2, respectively. Recently, Seyferth et al.<sup>5</sup> have attempted a synthesis of (1,1'-

(3) McCulloch, B. M.; Ward, D. L.; Woolins, J. D.; Brubak, C. H., Jr. *Organometallics* 1985, 4, 1425.

(4) Butler, I. R.; Cullen, W. R.; Kim, T.-J.; Rettig, S. J.; Trotter, J. *Organometallics* 1985, 4, 972.

(5) Seyferth, D.; Hames, T. G.; Rucker, T. G.; Cowie, M.; Dickson, R. S. *Organometallics* 1983, 2, 472.

(1) Watanabe, M.; Ichikawa, H.; Motoyama, I.; Sano, H. *Bull. Chem. Soc. Jpn.* 1983, 56, 3291.

(2) Whitesides, G.; Gaasch, J. F.; Stedronsky, E. S. *J. Am. Chem. Soc.* 1972, 94, 5258.